THE SELF-SIMILAR, TURBULENT, THREE-DIMENSIONAL WALL JET

Tim J. Craft, Brian E. Launder
Department of Mechanical Engineering
UMIST, P.O. Box 88,
Manchester, UK

ABSTRACT

Experiments of the 3-dimensional turbulent wall jet exhibit a rate of spread in the lateral direction significantly higher than that normal to the wall. The present contribution investigates the computed behaviour of the self-similar form of the jet, employing different levels of turbulence closure. It confirms that the rapid lateral spreading arises from the generation of streamwise vorticity, due to the anisotropy of the Reynolds stresses. However, even the best performing of the models tested overpredicts the spreading rate by some 50%. It is suggested that, because of the strong coupling between the axial and secondary flow, experiments require a significantly larger downstream distance to reach a fully-developed state than in the case of a 2-dimensional wall jet.

INTRODUCTION

The present paper considers the flow obtained when a turbulent jet is discharged along a smooth flat wall. Such wall jets are found in ventilation, film cooling and boundary-layer control applications, as well as being of relevance to the exhaust from jet engines prior to aircraft take-off.

Turbulent 3-dimensional wall jets have been studied experimentally by, among others, Newman et al. (1972); Davis and Winarto (1980); Fujisawa and Shirai (1989); Matsuda et al. (1990); Abrahamsson et al. (1997). One notable feature of the flow is that the jet exhibits a rate of spread parallel to the wall some five to seven times greater than that normal to the surface. The physical reasons for this highly asymmetric spreading are not fully understood though Newman et al. (1972) provided evidence to suggest that it was due to the generation of streamwise vorticity in the flow.

Some early calculations of the self-similar wall jet were reported by Kebede (1982), employing a high-Reynolds-number k-ε model. Although current work suggests that these earlier calculations were not entirely grid independent, Craft and Launder (1999), it confirms his finding that the linear k-ε model does not predict the large lateral spreading rate found experimentally.

The present work has adopted the same strategy as Kebede (1982) in that the transport equations have been transformed in order to allow the self-similar jet to be computed as a 2-dimensional problem. This enables one to avoid any concerns regarding numerical accuracy that may be present in predicting the full 3-dimensional shear flow. However, turbulence modelling, as well as computing power, has advanced over the years since Kebede's work, and the flow has thus been computed using both low and high-Reynolds-number stress transport models as well as the simpler eddy viscosity based k-ε model, in order to shed further light on the physical processes associated with the flow.

COMPUTATIONAL METHOD

Although the development of the wall jet would require the solution of a 3-dimensional problem, the present work obtains a solution just for the fully-developed jet via a 2-dimensional calculation. The method employed is an extension of that described by Kebede (1982), who predicted the flow using a high-Reynolds-number k-ε model with wall-functions and applied the thin shear layer approximations. In the present work, the method has been extended to include the solution of the modelled Reynolds-stress transport equations, including low-Reynolds-number models which resolve the near-wall sublayer. Calculations have also been performed which include the terms normally discarded in the thin shear layer approximation. However, the inclusion of these terms did not signifi-

cantly affect the results and, for clarity, the equations presented in this paper omit them.

Defining the coordinates x', y', z' as in Fig. 1, where z' is in the streamwise direction, y' the wall-normal and x' the lateral direction, similarity equations can be derived by non-dimensionalising all quantities using a reference length δ_r and velocity W_r:

$$x_i = x_i'/\delta_r \quad U_i = U_i'/W_r \quad \overline{u_i u_j} = \overline{u_i' u_j'}/W_r^2$$
$$\varepsilon = \varepsilon'/(W_r^3/\delta_r) \qquad P = (P' - P_\infty')/(\rho W_r^2)$$
$$\mu = \mu'/(W_r \delta_r) \tag{1}$$

With suitable definitions for δ_r and W_r the non-dimensional dependent variables are functions of only the cross-jet coordinates x and y. Applying these transformations to the Reynolds averaged Navier-Stokes equations then leads to the following:

$$\frac{\partial}{\partial x}(U^*U) + \frac{\partial}{\partial y}(V^*U) = -2(\beta+\alpha)WU - \frac{\partial P}{\partial x} - \frac{\partial}{\partial x}(\overline{u^2} - \beta\overline{uw}x) - \frac{\partial}{\partial y}(\overline{uv} - \beta\overline{uw}y) - 2\alpha\overline{uw} + \frac{\partial}{\partial x}\left(\nu\frac{\partial U}{\partial x}\right) + \frac{\partial}{\partial y}\left(\nu\frac{\partial U}{\partial y}\right) \tag{2}$$

$$\frac{\partial}{\partial x}(U^*V) + \frac{\partial}{\partial y}(V^*V) = -2(\beta+\alpha)WV - \frac{\partial P}{\partial y} - \frac{\partial}{\partial x}(\overline{uv} - \beta\overline{vw}x) - \frac{\partial}{\partial y}(\overline{v^2} - \beta\overline{vw}y) - 2\alpha\overline{vw} + \frac{\partial}{\partial x}\left(\nu\frac{\partial V}{\partial x}\right) + \frac{\partial}{\partial y}\left(\nu\frac{\partial V}{\partial y}\right) \tag{3}$$

$$\frac{\partial}{\partial x}(U^*W) + \frac{\partial}{\partial y}(V^*W) = -2(\beta+\alpha)WW - 2(\beta+\alpha)P + \beta\left(\frac{\partial Px}{\partial x} + \frac{\partial Py}{\partial y}\right) - \frac{\partial}{\partial x}(\overline{uw} - \beta\overline{w^2}x) - \frac{\partial}{\partial y}(\overline{vw} - \beta\overline{w^2}y) - 2\alpha\overline{w^2} + \frac{\partial}{\partial x}\left(\nu\frac{\partial W}{\partial x}\right) + \frac{\partial}{\partial y}\left(\nu\frac{\partial W}{\partial y}\right) \tag{4}$$

The modified convective velocities U^* and V^* are

$$U^* \equiv U - \beta W x \qquad V^* \equiv V - \beta W y \tag{5}$$

and the quantities α and β are defined as

$$\alpha \equiv \frac{\delta_r}{W_r}\frac{dW_r}{dz'} \qquad \beta \equiv \frac{d\delta_r}{dz'} \tag{6}$$

The continuity equation becomes

$$\frac{\partial U^*}{\partial x} + \frac{\partial V^*}{\partial y} + (\alpha + 2\beta)W = 0 \tag{7}$$

The two parameters α and β can be related to each other by considering the integral streamwise momentum balance, which yields:

$$\alpha + \beta = -\sigma/A \tag{8}$$

where

$$A \equiv \int\int (\rho W^2 + P)dxdy \tag{9}$$

$$\sigma \equiv 1/2 \int \mu \left.\frac{\partial W}{\partial y}\right|_{y=0} dx \tag{10}$$

The value of β, defining the streamwise coordinate stretching, can arbitrarily be taken as unity, and α is then updated each iteration of the solution process from equation (8), using the computed values of A and σ.

Similar transformations are applied to the transport equations for the Reynolds stresses and ε although, due to space constraints, these are not shown.

The subsequent equations are solved using a suitably modified version of the computer code STREAM (Lien and Leschziner, 1994), which is a finite volume solver employing a fully collocated grid arrangement. It adopts the SIMPLE algorithm of Patankar and Spalding (1972) (with Rhie and Chow (1983) interpolation to avoid chequerboarding) to maintain continuity, and the MUSCL scheme for convection (Van Leer, 1979). Computations were performed on rectangular domains with aspect ratios of up to 10 to accommodate the large lateral growth of the jet. Grids of up to 120 (lateral) $\times$ 80 (wall-normal) were employed, which ensured grid-independent solutions.

RESULTS AND DISCUSSION

The main purpose of the study has been to examine the physical mechanisms associated with the highly asymmetric spreading of the turbulent 3-dimensional wall jet. Consequently, computations have been made with a variety of models, including an eddy-viscosity scheme and several variants of Reynolds stress closure.

Table 1 shows the predicted spreading rates obtained with the Launder-Sharma k-ε model, which is seen to return a much too low lateral spreading rate, and to give a spreading rate ratio $(dx_{1/2}/dz)/(dy_{1/2}/dz)$ only slightly higher than that found in a laminar calculation.

Table 2 gives spreading rates predicted with 3 different Reynolds stress closures. Models 1 and 2 are both high-Reynolds-number models used with wall-functions, and differ only in the approximation made for the pressure-strain ϕ_{ij}. Model 1 simply comprises the widely used linear scheme:

$$\phi_{ij} = -c_1\varepsilon a_{ij} - c_2(P_{ij} - 1/3 P_{kk}\delta_{ij}) \tag{11}$$

where $a_{ij} \equiv \overline{u_i u_j}/k - 2/3\delta_{ij}$ and the production rate $P_{ij} \equiv -\overline{u_i u_k}\partial U_j/\partial x_k - \overline{u_j u_k}\partial U_i/\partial x_k$, whilst Model 2 adds the wall-reflection correction proposed by Craft and Launder (1992) to account for the presence of a rigid wall:

$$\phi_{ij}^w = \Big\{-0.08\frac{\partial U_l}{\partial x_k}\overline{u_l u_k}(\delta_{ij} - 3n_i n_j) + 0.4k\frac{\partial U_l}{\partial x_k}n_l n_k(n_i n_j - 1/3\delta_{ij})$$

	$dy_{1/2}/dz$	$dx_{1/2}/dz$	$\dot{x}_{1/2}/\dot{y}_{1/2}$
Expt. Abrahamsson et al. (1997)	0.065	0.32	4.94
Launder-Sharma prediction	0.079	0.069	0.88
Laminar calculation (at $Re = 300$)	0.043	0.023	0.54

Table 1: Wall-jet spreading rate with a linear EVM and for a laminar jet.

	$dy_{1/2}/dz$	$dx_{1/2}/dz$	$\dot{x}_{1/2}/\dot{y}_{1/2}$
Expt. Abrahamsson et al. (1997)	0.065	0.32	4.94
Model 1	0.081	0.079	0.97
Model 2	0.053	0.814	15.3
Model 3	0.060	0.51	8.54

Table 2: Wall-jet spreading rate with Reynolds stress closures.

$$-0.1a_{lm}\left(\frac{\partial U_k}{\partial x_m}n_l n_k \delta_{ij} - {}^3\!/_2 \frac{\partial U_i}{\partial x_m}n_l n_j - {}^3\!/_2 \frac{\partial U_j}{\partial x_m}n_l n_i\right)\Big\} \frac{l}{2.5y} \qquad (12)$$

where l is the turbulence lengthscale $k^{3/2}/\varepsilon$, $\underline{n}$ is the unit vector normal to the wall, and y the distance to the wall. Closure is completed by assuming local isotropy and the generalized gradient diffusion hypothesis for transport.

From Table 2 it can be seen that Model 1 gives spreading rates only a little different from those obtained with the k-ε model. However, the inclusion of equation (12) increases the spreading rate ratio by an order of magnitude, giving a value three times as high as the measurements of Abrahamsson et al. (1997). Model 3, also shown in Table 2, is the two-component limit (TCL) model developed at UMIST over the past 12 years, the particular form employed here being that of Craft (1998). This is a low-Reynolds-number stress model, which does not include additional wall-reflection terms, but is designed to be compatible with the two-component limit (Lumley, 1978) to which turbulence reduces at a wall. This model again predicts a large difference between lateral and wall-normal spreading rates, although in this case the ratio is closer to, but still significantly higher than, that found experimentally.

The non-dimensional profiles of the streamwise velocity, taken through the symmetry plane $x = 0$, (not shown) show little difference between the 3 RSM's. However, the profiles taken along the horizontal plane through the position of maximum velocity, plotted against distance $x/y_{1/2}$ in Fig. 2, show a large variation, in accordance with the predicted spreading rates. Figure 3 shows contours of the mean streamwise velocity computed with Model 3, compared to the experiments of Newman et al. (1972). Although the computed lateral width of the jet is clearly larger than in the experiments, the qualitative shape of the contours is encouragingly similar.

Davis and Winarto (1980) had suggested that the large ratio of lateral to normal spreading rates was due to asymmetric diffusion since turbulent velocity fluctuations parallel to the wall were much higher than normal to this surface. To test this hypothesis, a further calculation was performed, using the RSM of Model 2, retaining the Reynolds stresses in the streamwise momentum equation, but representing them via the eddy-viscosity formulation in the cross-stream U and V equations. This calculation led to a lateral spreading rate only slightly higher than that returned by the k-ε model (with a ratio $\dot{x}_{1/2}/\dot{y}_{1/2} \approx 1$), indicating that this is not the mechanism controlling the highly asymmetric spreading rates.

The predicted velocity field (with Model 3) in the cross-stream plane, Fig. 4, shows that fluid is entrained normal to the wall and deflected laterally. Profiles of the lateral velocity in a horizontal plane through the position of maximum streamwise velocity are shown in Fig. 5, confirming that the higher values of U/W_m (associated with greater streamwise vorticity) are returned by those models having larger lateral spreading rates.

To shed light on the coupling between the streamwise vorticity and the large lateral spreading rate, it is instructive to consider the transport equation for the vorticity Ω_z:

$$\begin{aligned}\frac{D\Omega_z}{Dt} &= \Omega_x\frac{\partial W}{\partial x} + \Omega_y\frac{\partial W}{\partial y} + \Omega_z\frac{\partial W}{\partial z} \\ &\quad + \frac{\partial^2}{\partial x \partial y}(\overline{v^2} - \overline{u^2}) + \frac{\partial^2 \overline{uv}}{\partial x^2} + \frac{\partial^2 \overline{uv}}{\partial y^2} \\ &\quad + \nu\left(\frac{\partial^2 \Omega_z}{\partial x^2} + \frac{\partial^2 \Omega_z}{\partial y^2}\right) \qquad (13)\end{aligned}$$

From equation (13) it is clear that the vorticity could be generated either by the anisotropy of the Reynolds stresses (as it is in turbulent flow through straight non-axisymmetric ducts) or by the stretching/bending of vortex lines. However, this latter mechanism is not significant in the fully-developed flow since the k-ε model predictions fail to capture the high lateral spreading rate of the 3-dimensional jet.

Further confirmation of the role of the Reynolds stresses in generating the streamwise vorticity comes from a consideration of the predictions obtained with Model 1. Without wall-reflection terms, this linear model returns almost equal values for $\overline{u^2}$ and $\overline{v^2}$ (since the linear ϕ_{ij} of Eq. (11) redistributes the streamwise normal stress equally into the other two components). The term involving $(\overline{v^2} - \overline{u^2})$ in Eq. (13) would thus be expected to make a negligible contribution in these predictions. From Table 2 it can be seen that Model 1 returns a very low lateral spreading rate. We may thus conclude that, as in non-circular duct flows, it is the anisotropy of the Reynolds stresses in Eq. (13) which is primarily responsible for generating the streamwise vorticity.

The above findings highlight the importance of this flow as one that can clearly discriminate between different models, and suggests that even the most elaborate of those tested may need further refinement to improve its performance. However, the computation scheme employed only returns the asymptotic self-preserving solution. One thus needs to examine whether the experimental measurements have actually reached such a state. It is known that in other shear flows, the coupling between axial velocity and vorticity can lead to very large development lengths being necessary before a fully-developed state is attained (eg. Cheah et al., 1993). There is also some evidence from parallel work reported at this meeting on the corresponding case of a 3-dimensional free-surface jet (Craft et al., 1999). In this case, the development of the jet has been simulated using a full 3-dimensional solver and it was found that, although the predictions of Model 3 were in reasonable agreement with the available measurements up to around 40 diameters, the computed fully-developed state had not been achieved at this point, but would appear to require a significantly longer development distance.

In the case of the wall jet, the most recent measurements of Abrahamsson et al. (1997) extend to around 80 diameters, whilst the data of Fujisawa and Shirai (1989), which do extend further, could be interpreted as showing a continued downstream growth of the spreading rate (though they were not reported in such terms by the authors). A full 3-dimensional calculation of the development over this distance would, of course, require substantial computer resources. In an attempt to address this question of how rapidly the jet develops, a numerical solver has thus been set up which solves the developing jet in a plane-by-plane manner, marching downstream in a parabolic fashion. This allows one to employ a solution domain which increases in size as the solution progresses, ensuring that adequate resolution of the flow is obtained at all stations.

Initial results of the developing jet have been obtained employing Model 3 in its high-Reynolds-number form, with wall-functions to account for the near-wall viscous-affected region, and the predicted development of the lateral and wall-normal spreading rates are shown in Fig. 6, together with the self-similar values returned by the same model. The computations have so far extended to 75 jet diameters downstream at which point, although the wall-normal spreading rate is close to its asymptotic value, the lateral spreading rate can be seen to be still growing. It is interesting to note also that at this location the predicted ratio of lateral to wall-normal spreading rates is around 5.4, in much closer accord with the experimental measurements than is the asymptotic value. The figure suggests that the predicted asymptotic state will not be reached until significantly further downstream than experimental measurements have been taken. Further calculations are planned to confirm this.

CONCLUSIONS

This study of the self-similar 3-dimensional turbulent wall jet has established that the exceptionally high rate of spread parallel to the wall is due to the creation of streamwise vorticity by the anisotropy of the Reynolds stress field. While this is the same mechanism that is responsible for secondary motions in straight, non-axisymmetric ducts, the value of the peak secondary velocities in the present case is an order of magnitude larger than found in ducts.

While Reynolds stress closures should, in principle, be able to reproduce the phenomenon, both models considered here (Models 2 and 3) lead to appreciably higher rates of spread than measured (Table 2). Nevertheless, the TCL model is in much closer agreement with the data of Abrahamsson et al. (1997) than the Basic model, despite no near-wall correction being employed.

Finally, given that streamwise vorticity builds up only slowly and is strongly coupled with the streamwise velocity, we question whether any of the experimental data have in fact achieved the asymptotic state. Several pointers suggest that the fully developed state has, indeed, not been reached, including the present preliminary computations of developing flow.

Acknowledgements

T.J. Craft acknowledges with gratitude the support of The Royal Society of London through a University Research Fellowship. Prof. M.A. Leschziner and Dr. F.-S. Lien kindly made available a copy of the basic STREAM code used in this study. Authors are listed alphabetically.

REFERENCES

Abrahamsson, H., Johansson, B., and Löfdahl, L., 1997, "An investigation of the turbulence field in the fully developed three-dimensional wall-jet," Tech. Rep. Internal Report 97/1, Chalmers University of Technology, Sweden.

Cheah, S. C., Cheng, L., Cooper, D., and Launder, B. E., 1993, "On the structure of turbulent flow in spirally fluted tubes," *Proc. 5th International Symposium on Refined Flow Modelling and Turbulence Measurements*, Paris.

Craft, T. J., 1998, "Developments in a low-Reynolds-number second-moment closure and its application to separating and reattaching flows," *Int. J. Heat Fluid Flow*, vol. 19, pp. 541–548.

Craft, T. J., Kidger, J. W., and Launder, B. E., 1999, "The development of 3-dimensional, turbulent, surface jets," *Turbulence and Shear Flow Phenomena - 1*, Begell House, New York.

Craft, T. J. and Launder, B. E., 1992, "New wall-reflection model applied to the turbulent impinging jet," *AIAA J.*, vol. 30, p. 2970.

Craft, T. J. and Launder, B. E., 1999, "The self-preserving, three-diemnsional turbulent wall jet," In preparation.

Davis, M. R. and Winarto, H., 1980, "Jet diffusion from a circular nozzle above a solid plane," *J. Fluid Mech.*, vol. 101, pp. 201–221.

Fujisawa, N. and Shirai, H., 1989, "Mean flow and turbulence characteristics of three-dimensional wall jet along plane surface," *Trans. Japan Soc. Aero. Space Sci.*, vol. 32, pp. 35–46.

Kebede, W., 1982, "Numerical study of the self-preserving three-dimensional wall-jet," M.Sc. Dissertation, Faculty of Technology, University of Manchester.

Lien, F.-S. and Leschziner, M. A., 1994, "A general non-orthogonal finite-volume algorithm for turbulent flow at all speeds incorporating second-moment turbulence-transport closure," *Comp. Meth. Appl. Mech. Eng.*, vol. 114, pp. 123–167.

Lumley, J. L., 1978, "Computational modelling of turbulent flows," *Adv. Appl. Mech.*, vol. 18, p. 123.

Matsuda, H., Iida, S., and Hayakawa, M., 1990, "Coherent structures in a three-dimensional wall jet," *ASME J. Fluids Engineering*, vol. 112, pp. 462–467.

Newman, B. G., Patel, R. P., Savage, S. B., and Tjio, H. K., 1972, "Three dimensional wall jet originating from a circular orifice," *Aero. Quarterly*, vol. 23, pp. 188–200.

Patankar, S. V. and Spalding, D. B., 1972, "A calculation procedure for heat, mass and momentum transfer in three-dimensional parabolic flows," *Int. J. Heat Mass Transfer*, vol. 15, p. 1787.

Rhie, C. M. and Chow, W. L., 1983, "Numerical study of the turbulent flow past an airfoil with trailing edge separation," *AIAA J.*, vol. 21, pp. 1525–1532.

Van Leer, B., 1979, "Towards the ultimate conservation difference scheme V, a second-order sequel to Godunov's method," *J. Comput. Phys.*, vol. 32, p. 101.

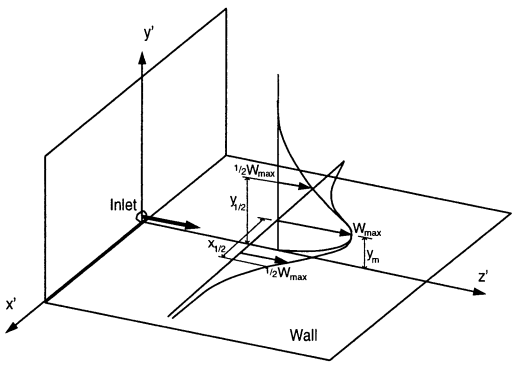

Figure 1: Schematic diagram of the 3-dimensional wall jet.

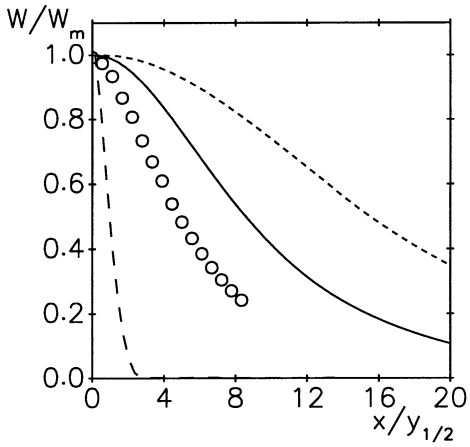

Figure 2: Profiles of mean streamwise velocity through the position of maximum velocity. —— Model 3; - - - Model 2; – – Model 1; Symbols, experiments of Abrahamsson et al. (1997).

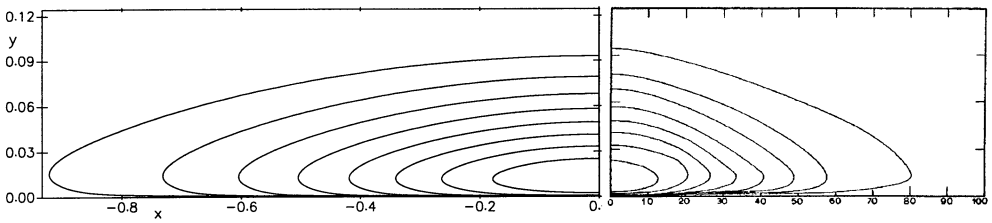

Figure 3: Contours of predicted (left) and measured (Newman et al., 1972, right) streamwise velocity.

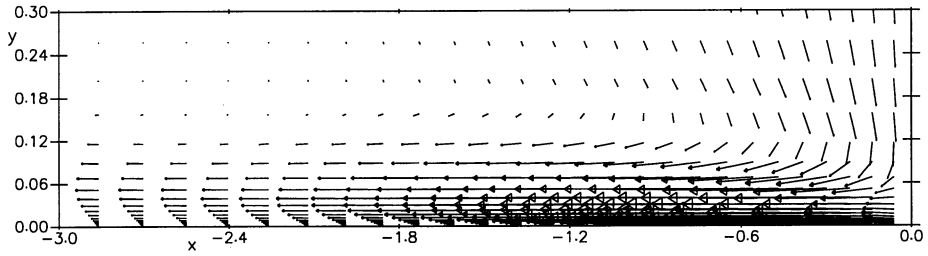

Figure 4: Predicted velcity field in the cross-stream plane.

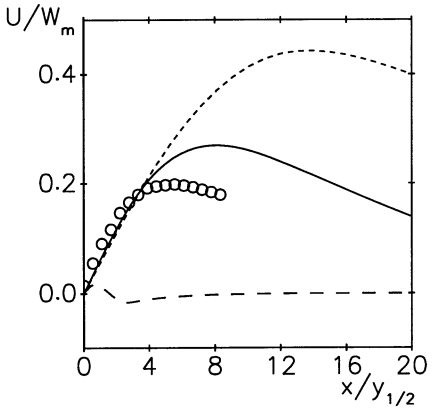

Figure 5: Profiles of mean lateral velocity through the position of maximum velocity. —— Model 3; - - - Model 2; – – Model 1; Symbols, experiments of Abrahamsson et al. (1997).

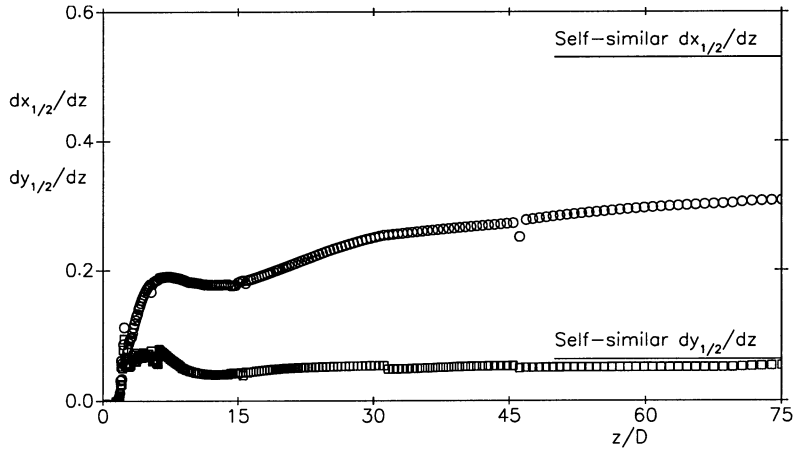

Figure 6: Predicted development of spreading rates in the wall-jet with Model 3. Circles: $dx_{1/2}/dz$, Squares: $dy_{1/2}/dz$